



Determination of zenith hydrostatic delay and its impact on GNSS-derived integrated water vapor

Xiaoming Wang^{1,2}, Kefei Zhang^{2,3}, Suqin Wu², Changyong He², Yingyan Cheng⁴, and Xingxing Li⁵

¹Academy of Opto-Electronics, Chinese Academy of Sciences, Beijing 100094, China

²Satellite Positioning for Atmosphere, Climate and Environment (SPACE) Research Centre, School of Science, Mathematical and Geospatial Sciences, RMIT University, Melbourne, Australia

³School of Environment Science and Spatial Informatics, China University of Mining and Technology, Xuzhou, China

⁴Institute of Geodesy and Geodynamics, Chinese Academy of Surveying and Mapping, Beijing, China

⁵Helmholtz-Zentrum Potsdam, Deutsches GeoForschungsZentrum GFZ, Brandenburg, Germany

Correspondence to: Kefei Zhang (kefei.zhang@rmit.edu.au)

Received: 4 August 2016 – Discussion started: 16 August 2016

Revised: 8 June 2017 – Accepted: 22 June 2017 – Published: 7 August 2017

Abstract. Surface pressure is a necessary meteorological variable for the accurate determination of integrated water vapor (IWV) using Global Navigation Satellite System (GNSS). The lack of pressure observations is a big issue for the conversion of historical GNSS observations, which is a relatively new area of GNSS applications in climatology. Hence the use of the surface pressure derived from either a blind model (e.g., Global Pressure and Temperature 2 wet, GPT2w) or a global atmospheric reanalysis (e.g., ERA-Interim) becomes an important alternative solution. In this study, pressure derived from these two methods is compared against the pressure observed at 108 global GNSS stations at four epochs (00:00, 06:00, 12:00 and 18:00 UTC) each day for the period 2000–2013. Results show that a good accuracy is achieved from the GPT2w-derived pressure in the latitude band between -30 and 30° and the average value of 6 h root-mean-square errors (RMSEs) across all the stations in this region is 2.5 hPa. Correspondingly, an error of 5.8 mm and 0.9 kg m^{-2} in its resultant zenith hydrostatic delay (ZHD) and IWV is expected. However, for the stations located in the mid-latitude bands between -30 and -60° and between 30 and 60° , the mean value of the RMSEs is 7.3 hPa, and for the stations located in the high-latitude bands from -60 to -90° and from 60 to 90° , the mean value of the RMSEs is 9.9 hPa. The mean of the RMSEs of the ERA-Interim-derived pressure across at the selected 100 stations is 0.9 hPa, which will lead to an equivalent error of 2.1 mm and 0.3 kg m^{-2} in the ZHD and IWV, respectively, determined

from this ERA-Interim-derived pressure. Results also show that the monthly IWV determined using pressure from ERA-Interim has a good accuracy – with a relative error of better than 3 % on a global scale; thus, the monthly IWV resulting from ERA-Interim-derived pressure has the potential to be used for climate studies, whilst the monthly IWV resulting from GPT2w-derived pressure has a relative error of 6.7 % in the mid-latitude regions and even reaches 20.8 % in the high-latitude regions. The comparison between GPT2w and seasonal models of pressure–ZHD derived from ERA-Interim and pressure observations indicates that GPT2w captures the seasonal variations in pressure–ZHD very well.

1 Introduction

Water vapor as a principal atmospheric parameter is a central component in both Earth's energy budget and water cycle. Accurate knowledge of water vapor is not only vital for weather forecasting but also an important independent data source for global climate studies. For the last decade, the Global Navigation Satellite System (GNSS) has been used as an emerging and robust tool for remotely sensing integrated water vapor (IWV) for the monitoring of the real-time IWV variations in the atmosphere (Schneider et al., 2010; Rohm et al., 2014; Zhang et al., 2015; Li et al., 2014, 2015; Guerova et al., 2016) or the studies of climate (Nilsson and Elgered, 2008; Jin and Luo, 2009; Vonder Haar et al., 2012; Ning

and Elgered, 2012) due to its 24 h availability, high accuracy, global coverage, high resolution and low cost. The atmospheric parameter directly estimated from GNSS measurements is the GNSS signal's tropospheric zenith total delay (ZTD) which can be effectively divided into the zenith hydrostatic delay (ZHD) and the zenith wet delay (ZWD). The ZHD can be accurately determined using the surface pressure observed by meteorological sensors. The GNSS-derived IWV over a station can then be obtained by multiplying the ZWD with a conversion factor which is a function of the water-vapor-weighted mean temperature T_m over the station. The T_m can be determined using one of the following three methods: (1) temperature and humidity profiles from either radiosonde observations or atmospheric reanalysis datasets (Wang et al., 2005, 2016a); (2) the relationship between surface temperature T_s and the water-vapor-weighted mean temperature T_m (Bevis et al., 1992, 1994; Ross and Rosenfeld, 1997); and (3) a blind model developed from atmospheric reanalysis products (Yao et al., 2012, 2015; Böhm et al., 2015).

Motivated by our early research (Wang et al., 2016a), it is vital to assess the performance of different methods for determining the ZHD on a global scale, which is essential in the development of a reliable global long-term IWV time series for climate studies. Although the ZHD can be accurately obtained from surface pressure observations, few GNSS stations were installed with meteorological sensors back in the 1990s since these stations were established mainly for precise positioning and navigation applications. Therefore, the lack of meteorological data (i.e., pressure) at these stations is a serious issue for the use of these historical GNSS data for global climate studies. To address this issue, an alternative method is to use pressure derived from a global atmospheric reanalysis (e.g., European Centre for Medium-Range Weather Forecasts Reanalysis, ERA-Interim; Dee et al., 2011) or a blind model (e.g., Global Pressure and Temperature 2 wet, GPT2w; Böhm et al., 2015). In this study, the errors in the pressure derived from these two approaches are investigated and the impact of these errors on the subsequent ZHD and IWV determination has also been studied.

For the performance assessment of these two methods, the ERA-Interim-derived pressure (using two computation methods) and the GPT2w-derived pressure are compared against the surface pressure measured at the 108 global GNSS stations during the period 2000–2013. To determine the pressure at a specific station from the ERA-Interim, first it is necessary to vertically extrapolate the pressure at surrounding grids on the nearest pressure level to the height of the station. Then, the pressure at this station is either horizontally interpolated from the obtained four surrounding grids (four-point method) or set to the pressure at the nearest grid at the same height (one-point method, no horizontal interpolation). In this study, the impact of the error in these pressure values on the ZHD is evaluated by comparing the resultant ZHD against the ZHD derived from the surface pressure measured. Similarly, the impact of these errors on the IWV is also as-

essed. As stated in the product requirement document from the EIG EUMETNET GNSS Water Vapour Programme (Offiler, 2010), the accuracy of IWV for the Global Climate Observing System (GCOS) required is better than 3 kg m^{-2} . The “breakthrough” and “goal” accuracy are 1.5 and 1 kg m^{-2} , respectively. Since a 1 hPa error in pressure will lead to a 2.3 mm error in its resultant ZHD and about 0.35 kg m^{-2} in its resultant IWV, the errors of pressure and ZHD should be under 2.9 hPa and 6.6 mm, respectively, to ensure a better than 1 kg m^{-2} accuracy for their resultant IWV. Bock et al. (2013) also pointed out that for climate monitoring it is necessary to achieve a 3% or better accuracy from GNSS-derived IWV. Since for climate studies the accuracy of IWV (in terms of root-mean-square error, RMSE) can be obtained by averaging observations of a site over a long period (e.g., a month), the error in IWV is studied not only for the four epochs of each day but also for the monthly mean.

2 Datasets and methods

2.1 Datasets

In this study, surface pressure observations provided by the Scripps Orbit and Permanent Array Center (SOPAC), ERA-Interim from ECMWF and the GPT2w model are used to investigate the performance of GPT2w and ERA-Interim in the determination of pressure. To investigate the impact of the error in pressure on the resultant IWV, the IWVs at 108 stations are calculated and analyzed with the ZTD reanalysis products provided by the Center for Orbit Determination in Europe (CODE).

2.1.1 Surface pressure observations and GNSS-derived ZTD

Recently, reprocessing of historical GNSS data has emerged as a new initiative in the world GNSS community, driven by the high demand of various new scientific studies. For example, CODE has reprocessed GNSS observations at 371 global IGS (International GNSS Service) stations for the period of 1994–2013 and made the results public to the science community (see ftp://ftp.unibe.ch/aiub/REPRO_2013/). Some of these centers have also collected meteorological observations at these IGS stations, e.g., the Scripps Orbit and Permanent Array Center (see <http://garner.ucsd.edu/pub/met/>). In this study, the meteorological observations provided by the SOPAC and the ZTD results provided by CODE are used to determine ZHD and IWV.

Surface pressure provided by SOPAC is used to validate the performance of ERA-Interim- and GPT2w-derived surface pressure. However, as suggested by previous studies (Wang et al., 2007; Heise et al., 2009; Bianchi et al., 2016), meteorological data provided by IGS need to be rigorously screened before they are used to calculate IWV. In this study, the pressure values from 131 stations are screened carefully

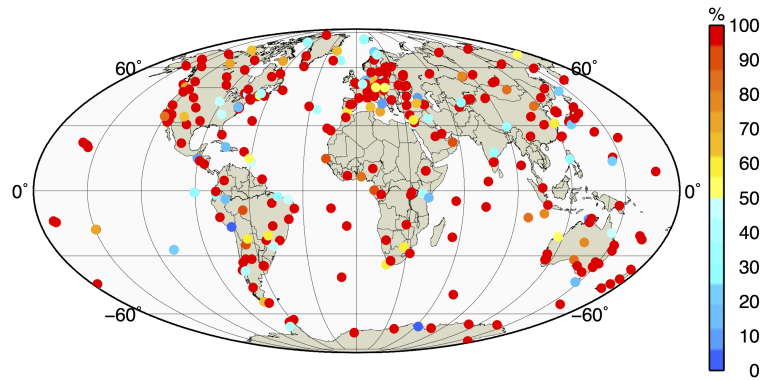


Figure 1. Percentage of the missing surface pressure observations compared to the GNSS-derived ZTD at 371 IGS stations for the period of 2000–2013. Results indicate that no pressure observations are recorded at 67 % of stations, and the percentage of missing data is smaller than 25 % only at 6 % of stations.

based on the method suggested by Wang et al. (2007) to prevent those poor-quality surface pressure observations from being used. Firstly, the time series of pressure at all 131 stations are visually checked carefully to delete stations at which the pressure values have obvious large noises or offsets (which might be caused by the change of pressure sensors). This leads to 23 stations being deleted, and the remaining 108 stations (see the Supplement) are used in this study. Then, the pressure values at these 108 stations are further checked for detecting and excluding unrealistic values out of the range between 550 and 1100 hPa. The third and also the last step is identifying those pressure values that depart from the mean value of more than three standard deviations at each station, which leads to about 0.5 % of the data being detected and excluded from use. It also needs to be noted that the IGS surface pressure observations are not homogenized, and they are therefore not suitable for long-term climate studies.

Since the time series of both the GNSS-derived ZTDs and the pressure measured contain gaps, the missing-data rates of these time series need to be investigated. As a result, a comparison between the meteorological observations and ZTDs over 371 global stations at four epochs (00:00, 06:00, 12:00, 18:00 UTC) of each day during the whole period of 2000–2013 is carried out. The missing-data rates of pressure observations compared to the ZTDs are shown in Fig. 1, which indicates that at most stations only few meteorological observations were recorded. Statistical results indicate that the percentage of missing data smaller than 25 % happens only at 6 % of the stations and there were no pressure observations recorded at 67 % of the stations. Thus, a reliable alternative method for obtaining surface pressure is needed for the determination of IWV from historical GNSS observations.

2.1.2 ERA-Interim

The global atmospheric reanalysis datasets used are from ERA-Interim, which is produced by the European Centre

for Medium-Range Weather Forecasts (ECMWF; Dee et al., 2011) and has been widely used for global climate studies. The ERA-Interim data cover the period from 1 January 1979 onwards, and near-real-time information is also generated. All these are available at 00:00, 06:00, 12:00 and 18:00 UTC of each day. The spatial resolution of the ERA-Interim is approximately 80 km (reduced Gaussian grid N128) in horizontal and at 37 vertical pressure levels. The ERA-Interim is used to determine the conversion factor Π and compute surface pressure in this study.

2.1.3 GPT2w

The blind model selected is GPT2w (Böhm et al., 2015), which provides the mean value plus annual and semiannual amplitudes of the pressure. Böhm et al. (2007) first developed a blind model, called GPT, based on 3-year monthly-mean profiles of pressure and temperature from the ECMWF 40-year reanalysis data (ERA40) for providing pressure and temperature at any site in the vicinity of the Earth's surface. Lagler et al. (2013) then developed GPT2 by improving and combining GPT and Global Mapping Function using data of 10-year (2001–2010) 37-month-mean pressure levels from ERA-Interim. The latest GPT2w (Böhm et al., 2015) is an extension of GPT2 with an improved capability in the determination of zenith wet delays in the blind mode. The GPT2w model with the gridded input file is available at <http://ggosatm.hg.tuwien.ac.at/DELAY/SOURCE/GPT2w/>. To determine the pressure value at a GNSS station, the GPT2w model first determines the pressure values at four nearest grid points surrounding the station based on a $1^\circ \times 1^\circ$ external grid file. Then, the pressure values at these four grids at the height of the station are calculated using an vertical exponential trend coefficient related to the inverse of the virtual temperature (Böhm and Schuh, 2013). Lastly, the pressure at the GNSS station is linearly interpolated from the above four pressure values

2.2 Methods for interpolating pressure data from ERA-Interim

Since one nearest pressure level to a GNSS station is used to compute the pressure at this station, the vertical distance between pressure level and this GNSS station will probably affect the accuracy of the pressure derived from ERA-Interim due to its limited vertical resolution. We calculated the mean value of the height differences between the GNSS station and four surrounding grids at the nearest pressure level and studied the relationship between the errors in ERA-Interim-derived pressure and this mean height difference. Results indicate that the difference between the GNSS station and its nearest pressure level is between 26 and 181 m at all 108 stations. Additionally, the error (bias and RMSE) in ERA-Interim-derived pressure does not show an obvious dependence on this height difference. For the height below 10 km, the height between two pressure levels in ERA-Interim is about 500 m, which means we can always find the nearest pressure level to a GNSS station with a height difference less than 250 m. Therefore, the vertical resolution of ERA-Interim seems sufficient for the pressure interpolation for the GNSS station. However, in mountainous areas where the pressure levels in ERA-Interim are below the actual terrain, the pressure values on these levels are extrapolated from the model and the results may not be in a good accordance with pressure observations. When ERA-Interim is used to obtain the pressure at a GNSS station, either the pressure from the nearest grid (one-point method) or four surrounding grids (four-point method) and also on the nearest pressure level is used.

2.2.1 One-point method

The one-point method uses meteorological data at an ERA-Interim grid that is closest to the GNSS station to compute the pressure P_s for the station (ICAO, 1993) by

$$P_s = p_c \left[\frac{T_c - \gamma (H_s - H_c)}{T_c} \right]^{\frac{g \cdot M}{R \cdot \gamma}}, \quad (1)$$

where p_c , T_c and H_c are the air pressure, temperature (in K) and height (in m) of the nearest ERA-Interim grid point (on the nearest pressure level), respectively; $\gamma = 0.0065 \text{ K m}^{-1}$ is the standard temperature lapse rate; H_s is the station height; $M = 0.0289644 \text{ kg mol}^{-1}$ is the molar mass of dry air; $R = 8.31432 \text{ (N m (mol K)}^{-1})$ is the ideal gas constant and g is a gravitational parameter which can be determined by

$$g = 9.8063 \cdot \left\{ 1 - 10^{-7} \frac{H_c + H_s}{2} [1 - 0.0026373 \cdot \cos(2\varphi) + 5.9 \times 10^{-6} \cdot \cos^2(2\varphi)] \right\}, \quad (2)$$

where φ is the latitude of the GNSS station.

2.2.2 Four-point method

The four-point method uses the pressure values from the nearest pressure level at four neighboring grid points to determine the pressure for the GNSS station ($\varphi_s, \lambda_s, H_s$). Two procedures need to be carried out: a vertical computation procedure and a horizontal computation procedure. The vertical computation uses pressure values at the nearest pressure level to determine four pressure values, p_i ($i = 1, 2, 3, 4$), at four nearby grid points at the height of the GNSS station using Eqs. (1) and (2). After p_i ($i = 1, 2, 3, 4$) is obtained, the next step is to horizontally interpolate the pressure value at the GNSS station ($\varphi_s, \lambda_s, H_s$) by

$$p_s = \sum_{i=1}^4 \overline{w}_i p_i, \quad (3)$$

where \overline{w}_i is a weighting coefficient computed by

$$\overline{w}_i = \frac{w_{*i}}{w_{*1} + w_{*2} + w_{*3} + w_{*4}} \quad (i = 1, 2, 3, 4), \quad (4)$$

where w_{*i} is a weighting coefficient for the i th grid point calculated by

$$w_{*i} = \psi_i^{-1}, \quad (5)$$

where ψ_i is the spherical distance between the grid point and the GNSS station.

2.3 Computation of ZHD and IWV

One of the most commonly used methods to obtain the ZHD is using the Saastamoinen formula, which is a function of surface pressure (Saastamoinen, 1972; Elgered et al., 1991; Niell et al., 2001). Davis et al. (1985) pointed out that the uncertainty in the ZHD obtained from the Saastamoinen formula was 0.5 mm, if uncertainties in the physical constants and the calculation of the mean value of gravity were taken into consideration. This magnitude of uncertainty will introduce an uncertainty of less than 0.1 kg m^{-2} in its subsequent IWV determination, which can be neglected.

Equations (6) and (7), developed by Elgered et al. (1991) based on the Saastamoinen formula, are adopted in this study to obtain the ZHD (in mm). These formulae have been widely used in many studies (Bevis et al., 1992; Bock and Doerflinger, 2001; Bokoye et al., 2003; Kleijer, 2004; Musa et al., 2011; Kumar et al., 2013; Norazmi et al., 2015).

$$\text{ZHD} = (2.2779 \pm 0.0024) P_s / f(\varphi H), \quad (6)$$

where P_s is the total pressure (in hPa) at the station's height (in km) and

$$f(\varphi, H) = 1 - 0.00266 \cdot \cos(2\varphi) - 0.00028H \quad (7)$$

accounts for the variation in the gravitational acceleration at the station with latitude φ and height H above a reference ellipsoid.

In the calculation of the IWV with Eq. (8), the ZTD provided by CODE and the conversion factor Π computed from the temperature and humidity profiles from the ERA-Interim are adopted.

$$\text{IWV} = \Pi \cdot \text{ZWD} = \Pi \cdot (\text{ZTD} - \text{ZHD}) \quad (8)$$

More details about the computation of Π have been published in Wang et al. (2016a), and here only a brief description of the calculation of Π is given. As a function of T_m , Π can be calculated using

$$\Pi = \frac{10^6}{\rho R_v \left[\frac{k_3}{T_m} + k_2' \right]}, \quad (9)$$

$$k_2' = k_2 - m k_1, \quad (10)$$

where ρ is the density of liquid water, R_v is the specific gas constant for water vapor, and m is the ratio of the molar masses of water vapor and dry air. The values of physical constants $k_1 = 77.60 \pm 0.05 \text{ K mbar}^{-1}$, $k_2 = 70.4 \pm 2.2 \text{ K mbar}^{-1}$ and $k_3 = 3.739 \pm 0.012 \cdot 10^5 \text{ K}^2 \text{ mbar}^{-1}$ are from the widely used formula for atmospheric refractivity (Bevis et al., 1994), and the constant k_2' derived from Eq. (10) was set to $22.1 \pm 2.2 \text{ K mbar}^{-1}$ as suggested by Bevis et al. (1994).

T_m in Eq. (9) is the water-vapor-weighted mean temperature (Davis et al., 1985) and is approximated as

$$T_m = \frac{\int \frac{P_v}{T} dz}{\int \frac{P_v}{T^2} dz} \approx \frac{\sum_{i=1}^N \frac{P_{vi}}{T_i} \Delta z_i}{\sum_{i=1}^N \frac{P_{vi}}{T_i^2} \Delta z_i}, \quad (11)$$

where P_v is the partial pressure (in hPa) of WV, T is the atmospheric temperature (in K) and i is the i th pressure level. P_v can be calculated using (Tetens, 1930)

$$P_{si} = 6.11 \times 10^{\left(\frac{7.5 \times T_i}{237.3 + T_i} \right)}, \quad (12)$$

$$P_{vi} = \frac{\text{rh}_i \cdot P_{si}}{100}, \quad (13)$$

where P_s is the saturated vapor pressure over water, rh is the relative humidity and T is the atmospheric temperature (in C).

3 Comparison and analysis

One possible error source for the determination of pressure from GPT2w and ERA-Interim is the representativeness error in this model due to the limited model resolution (Janjić and Cohn, 2006; Bock and Nuret, 2009). The representativeness error arises when the point observations can well represent small spatial scales but the model cannot, and this error may be extreme in complex mountainous terrain, where there is a mismatch between the model and actual terrain (Zhang et al., 2013). Although a previous study (Wilgan et al., 2015)

indicated that the one-point method may have a better performance than the four-point method in mountainous areas, this phenomenon was not confirmed in our study. To investigate the performance of the aforementioned methods in the determination of pressure and its impact on the resultant ZHD and IWV, the pressure, ZHD and IWV at 108 stations for the period 2000–2013 resulting from both GPT2w and ERA-Interim using the aforementioned two methods are compared against surface pressure measurements and their resultant ZHD and IWV.

3.1 Comparisons of 6 h pressure data

To investigate the performance of the GPT2w and ERA-Interim methods, the biases and RMSEs of the resultant pressures, ZHD and IWV at 108 stations for the period of 2010–2013 (using observed pressure as a reference) are computed. The pressure derived from the GPT2w model, the ERA-Interim with the one-point method and ERA-Interim with the four-point method are named as P_GPT2w, P_ERA1 and P_ERA4, respectively. Equation (14) shows the calculation of RMSE, which is a widely used measure of the differences between model-derived values and reference/true values such as the observed values.

$$\text{RMSE}(P_{\text{cal}}) = \sqrt{\frac{\sum_{i=1}^n (P_{\text{cal}}(i) - P_{\text{ref}}(i))^2}{n}}, \quad (14)$$

where P_{cal} is the pressure derived from GPT2w or ERA-Interim, P_{ref} is the reference pressure from observations and n is the number of pressure observations.

As indicated in Fig. 2, the RMSE of P_GPT2w is obviously latitude dependent and also obviously larger than that of both P_ERA1 and P_ERA4 at the same stations. For the 28 stations located in the low-latitude band between -30 and 30° , the RMSEs of P_GPT2w are in the range of 1.4 to 4.3 hPa and the mean of these 28 RMSEs is 2.5 hPa. For the 59 stations located in the mid-latitude bands of -30 to -60 and 30 to 60° , the RMSEs of P_GPT2w are in the range of 2.8 to 11.9 hPa with a mean of 7.3 hPa. For the 13 stations located in the high-latitude belts of -60 to -90 and 60 to 90° , the RMSEs are in the range of 7.8 to 12.4 hPa and the mean value reaches 9.9 hPa. Therefore, GPT2w has a far better performance in the low-latitude regions than in the other regions in the determination of surface pressure, and the error of the GPT2w-derived 6 h pressure data may be dominated by the spatial and temporal representativeness error in GPT2w.

Although, the RMSEs of P_ERA1 and P_ERA4 across the 108 stations are mostly under 2 hPa, there are still 8 stations (JOZ2, WHIT, WROC, OHIG, GOPE, BOR1, SOFI and WUHN) that have an RMSE larger than 2 hPa, and 7 out of these 8 stations have a bias larger than 1 hPa or smaller than -1 hPa. The large difference between the observed surface pressure and the pressure derived from ERA-Interim is probably caused by poor-quality observations at these stations. Therefore, these eight stations are not used in the fol-

Table 1. Mean values of the biases and RMSEs of 6 h pressure, ZHD and IWV derived from GPT2w and ERA-Interim for the 100 stations in low- (−30 to 30°), mid- (30 to 60° and −30 to −60°) and high-latitude (60 to 90 and −60 to −90°) regions for the period 2000–2013.

Method	Region	Number of stations	Pressure (hPa)		ZHD (mm)		IWV (kg m ^{−2})	
			Bias	RMSE	Bias	RMSE	Bias	RMSE
GPT2w	Low-latitude	28	−0.06	2.53	−0.14	5.77	0.03	0.94
	Mid-latitude	59	30.32	7.25	−0.73	16.50	0.11	2.55
	High-latitude	13	0.57	9.90	1.29	22.51	−0.21	3.33
ERA-Interim (one-point)	Low-latitude	28	−0.17	0.74	−0.69	1.84	0.11	0.30
	Mid-latitude	59	0.34	0.99	−0.97	2.30	0.15	0.36
	High-latitude	13	0.17	0.94	0.30	2.14	−0.04	0.31
ERA-Interim (four-point)	Low-latitude	28	−0.13	0.76	−0.30	1.73	0.05	0.28
	Mid-latitude	59	0.34	0.95	−0.78	2.16	0.12	0.34
	High-latitude	13	0.17	0.90	0.39	2.04	−0.05	0.30

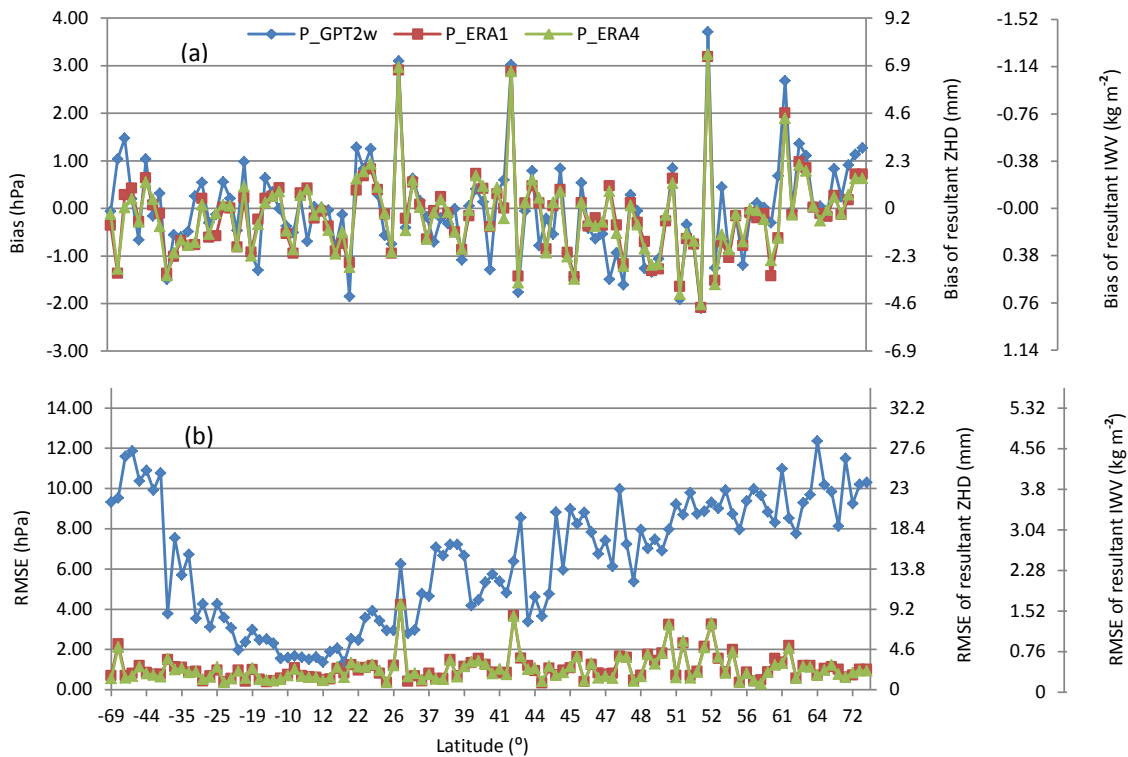


Figure 2. Distribution of biases (a) and RMSEs (b) of 6 h P_GPT2w, P_ERA1 and P_ERA4 with latitudes across 108 GNSS stations for the period of 2000–2013. IWV is integrated water vapor.

lowing sub-sections, i.e., only the remaining 100 stations (Table 1) are used to assess the performance of ERA-Interim and GPT2w in the determination of pressure.

It can be seen from Fig. 2a that there is no obvious correlation between the magnitudes of the biases (between −1 and 1 hPa at most stations) and the latitudes of stations for the pressure derived from GPT2w and ERA-Interim. Figure 2a also shows that the biases of the pressure obtained from all three methods are quite similar at most stations. As shown

in Fig. 2b, the results from the ERA-Interim using the two aforementioned computation methods have a similar accuracy. The RMSEs of both P_ERA1 and P_ERA4 are in the range of 0.2 to 4.0 hPa, and the mean values of these two sets of RMSEs are both about 0.7 hPa in the low-latitude region and around 1.1 hPa in the other regions. Figure 3 indicates that the distribution of both bias and RMSEs in all three sets of pressure has no obvious correlation with stations’ height. Therefore, the error in the ERA-Interim-derived pressure–

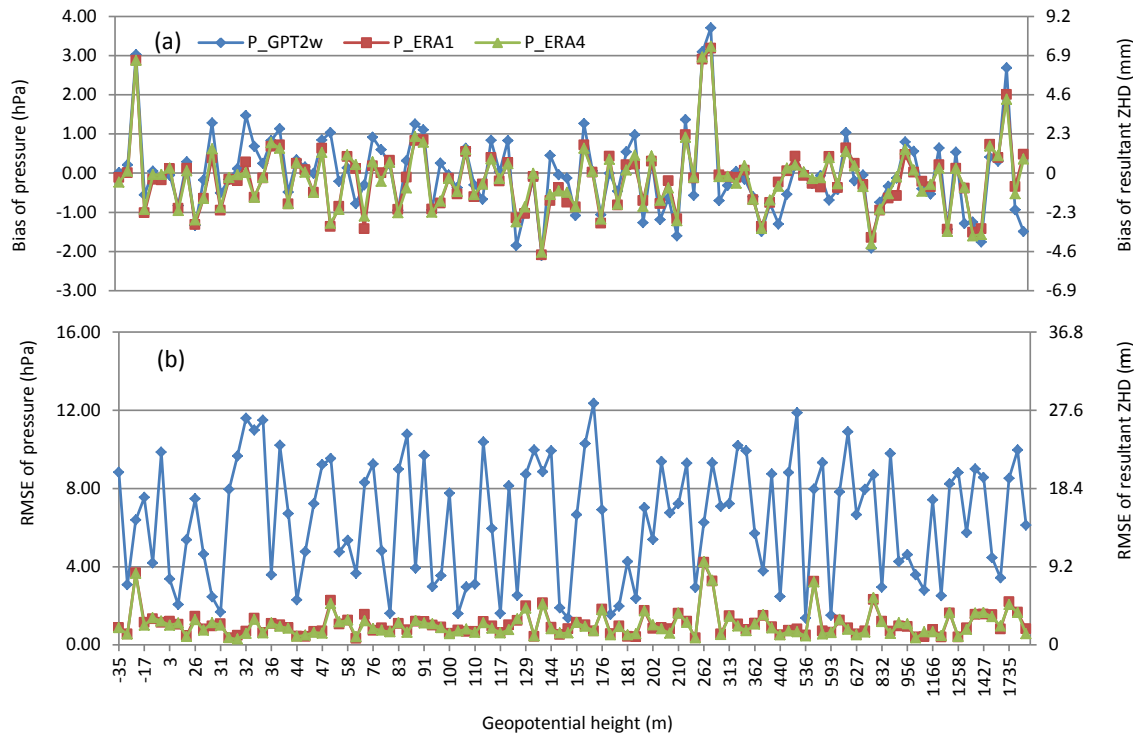


Figure 3. Distribution of biases (a) and RMSEs (b) of 6 h P_GPT2w, P_ERA1 and P_ERA4 with heights across 108 GNSS stations for the period of 2000–2013.

ZHD is not dominated by the spatial representativeness error in ERA-Interim.

As indicated by our results, except for the aforementioned eight stations that probably have poor-quality surface observations, the accuracies of the pressure derived from ERA-Interim at the remaining 100 stations are quite similar and they do not show any dependence on the latitude and height of stations. Therefore, the accuracy and spatial resolution of ERA-Interim seems sufficient for the determination of pressure on a global scale, and the model's representativeness error does not have an obvious impact on the resultant pressure. The similar accuracies of the P_ERA1 and P_ERA4 results indicate that if there are representativeness errors in ERA-Interim they tend to be similar in the one-point and four-point data. It is also likely that the differences between the ERA-Interim-derived pressure and observed pressure are dominated by the error in the observations rather than the error in the ERA-Interim model. However, the differences between the pressure derived from ERA-Interim and GPT2w are mainly caused by the differences of their spatial and temporal representativeness.

3.2 Comparison of 6 h and monthly pressure, ZHD and IWV

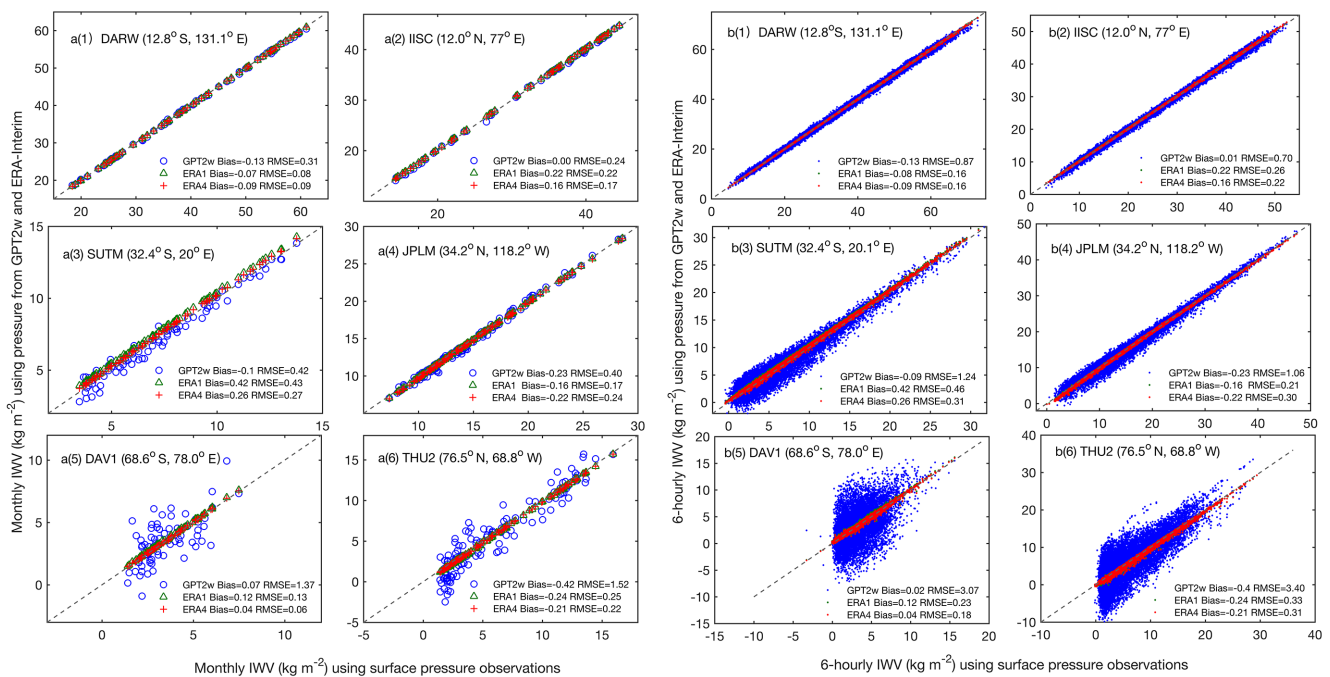
A 1 hPa error in determined pressure will lead to a 2.3 mm error in its resultant ZHD and about 0.35 kg m^{-2} in its re-

sultant IWV. Therefore, the characteristics of the spatial distribution of the errors in ZHD and IWV are quite similar to that in pressure. Table 1 (more details can be found in Supplement 1) shows the statistical results of the bias and RMSE of the pressure, ZHD and IWV derived from the abovementioned three methods for three latitudinal bands. One can see that the accuracies of the ZHD and IWV derived from ERA-Interim with the two aforementioned methods are quite similar and noticeably better than the accuracy of that derived from GPT2w. As listed in Table 1, the biases of the ERA-Interim-derived ZHD are within -1 to 1 mm and the RMSE is about 2 mm at these 100 stations. In terms of IWV, the RMSE of the ERA-Interim-derived IWV is about 0.3 kg m^{-2} on a global scale. However, the RMSEs of the GPT2w-derived ZHD and IWV reach 22.51 mm and 3.33 kg m^{-2} , respectively, in the high-latitude region, which are significantly larger than those in the low-latitude region.

Since for climate studies we are more interested in monthly mean data, the accuracy of monthly IWV is analyzed. The accuracy of monthly IWV calculated from GPT2w- and ERA-Interim-derived pressure is measured by the difference from the monthly IWV resulting from surface pressure observations (the latter is the reference). IWVs obtained from surface pressure P_GPT2w, P_ERA1 and P_ERA4 are named as IWV_GPT2w, IWV_ERA1 and IWV_ERA4, respectively. Table 2 (more details can be found in Supplement 2) shows the statistical results of the bias,

Table 2. Bias, RMSE and relative error of monthly I WV derived from GPT2w and ERA-Interim at 99 stations for the period 2000–2013.

Method	Region	Number of stations	Bias (kg m^{-2})	RMSE (kg m^{-2})	Relative error (%)
GPT2w	Low-latitude	28	0.03	0.41	1.53
	Mid-latitude	59	0.10	0.92	6.69
	High-latitude	12	-0.19	1.44	20.82
ERA-Interim (one-point)	Low-latitude	28	0.10	0.23	0.90
	Mid-latitude	59	0.15	0.26	1.96
	High-latitude	12	-0.02	0.18	2.52
ERA-Interim (four-point)	Low-latitude	28	0.04	0.20	0.77
	Mid-latitude	59	0.12	0.25	1.82
	High-latitude	12	-0.04	0.17	2.31

**Figure 4.** Scatter plots of the monthly mean of I WV (a1–a6) and 6 h I WV (b1–b6) determined using surface pressure observations (x axis) and I WV determined using pressure from GPT2w and ERA-Interim (y axis) for the period of 2000–2013 (ZTD from CODE is used in the computation of I WV).

RMSE and relative error of the monthly I WV derived from the aforementioned three methods at 99 stations. The relative error is calculated using $100 \cdot \text{RMS}/\text{I WV}$. It should be noted that the aforementioned eight stations with possible poor data quality and one station with a large amount of missing data, which therefore cannot be used to calculate the monthly mean result, are not used in Table 2. It can be seen that the error in both I WV_ERA1 and I WV_ERA4 is quite small, with an RMSE of about 0.23 kg m^{-2} on a global scale. The relative errors in both I WV_ERA1 and I WV_ERA4 in the low-latitude, mid-latitude and high-latitude regions are about 0.8, 1.9 and 2.5 %, respectively. The mean relative er-

ror of both I WV_ERA1 and I WV_ERA4 across all 99 stations is about 1.6 %. However, for I WV_GPT2w, the relative error is as high as 6.7 % in the mid-latitude regions and can even be up to 20.8 % in the high-latitude regions. Therefore, the monthly I WV calculated from ERA-Interim-derived pressure has a good accuracy, especially in the low- and mid-latitude regions; thus, it has the potential to be used for climate studies.

Figure 4a1–a6 shows the scatter plots between the monthly I WV derived from surface pressure (x axis) and I WV_GPT2w, I WV_ERA1 and I WV_ERA4 (y axis) at six stations in three latitude belts. As shown in this figure, both

monthly IWV_ERA1 and IWV_ERA4 do not contain obvious biases compared to the IWV derived from surface pressure observations. However, from the IWV_GPT2w result, obvious biases can be found at stations in mid- and high-latitude belts, especially at low IWV values. This is more obvious in the scatter plots for the 6 h IWV data as shown in Fig. 4b1–b6. The large error at low IWV values might be caused by the fact that GPT2w-derived pressure usually has a larger error in the cold season, when the IWV values are expected to be low. More discussion regarding this issue is presented in Sect. 3.4.

As shown in Table 2, the accuracies of monthly P_ERA1 and P_ERA4 are not dependent on the horizontal location indicating that the monthly pressure data from ERA-Interim are not dominated by the spatial representativeness error in ERA-Interim. The comparison between the statistical results in Tables 1 and 2 also shows that the error in the GPT2w-derived monthly pressure data is noticeably smaller than that in the 6 h pressure data derived from GPT2w. This implies that the error in the GPT2w-derived 6 h pressure is affected by the temporal representativeness error in GPT2w. Although the error in the ERA-Interim-derived monthly pressure data is also smaller than that in the 6 h pressure data, the improvements are not as significant as those of GPT2w.

3.3 Seasonal variation in pressure and ZHD

In this section, as shown in Eq. (15), seasonal models (annual and semiannual cycles) were fitted using the least squares estimation method from three sets of pressure (i.e., P_GPT2w, P_ERA1, P_ERA4 and surface pressure observations).

$$P = P_{\text{mean}} + a_1 \cdot \sin(t_i \cdot 2\pi) + b_1 \cdot \cos(t_i \cdot 2\pi) + a_2 \cdot \sin(t_i \cdot 4\pi) + b_2 \cdot \cos(t_i \cdot 4\pi), \quad (15)$$

where P_{mean} is the mean value (a_1 , b_1) and (a_2 , b_2) are the annual and semiannual amplitudes, respectively.

Figure 5 gives an example of the comparison among the ZHD derived from GPT2w and seasonal models from ERA-Interim and pressure observations at site QAQ1. Then, the temporal characteristics of the errors in the pressure and ZHD time series reconstructed using Eq. (15) are studied. As expected, the mean values of pressure and ZHD at a GNSS station are closely related to the station height. However, the annual amplitudes of the pressure and ZHD do not show a very strong dependence on the station height but vary by locations. For example, the amplitudes seem larger over stations in eastern Asia than that in western Europe. The semiannual amplitudes are much smaller than the annual amplitudes and thus are not discussed here. Figure 6 shows the annual amplitudes of the ZHD calculated from GPT2w, ERA-Interim and pressure observations at 76 stations (15 stations in low-latitude, 49 in mid-latitude and 12 in high-latitude belts) with a time span of more than 3 years, and the percentage of missing data is less than 50 % in observed pressure. It

shows that the annual amplitudes of these four sets of ZHDs show a very good agreement.

Next we compare the reconstructed seasonal models (including fitted annual and semiannual components) from models and observations. As shown in Fig. 7, the biases of pressure from the P_GPT2w and seasonal models of P_ERA1/P_ERA4 are in a range of -2 to 2 hPa, and the RMSE values are under 2 hPa at most stations. The biases of ZHD from the P_GPT2w and seasonal models of ZHD from ERA-Interim are in a range of -4.6 to 4.6 mm and the RMSE values are under 4.6 mm at most stations. Since the seasonal models estimated from P_GPT2w, P_ERA1 and P_ERA4 can be regarded as consistent in temporal scale, the differences among these models are mainly caused by the differences in their spatial resolutions. Since the accuracies of these three seasonal models are similar and agree well with the seasonal models estimated from the time series of pressure observations, the error in the seasonal models from GPT2w-derived pressure is not dominated by its spatial representativeness error.

3.4 Seasonal variations in the errors of the pressure and ZHD

To further study the characteristics of the error in pressure and ZHD derived from GPT2w and ERA-Interim, the amplitudes of the annual cycles in the errors of the P_GPT2w and P_ERA1–P_ERA4 time series were calculated based on the 6 h data at the aforementioned 76 stations, and the mean values of the annual amplitudes are around 0.5 hPa (P_GPT2w) and 0.2 hPa (P_ERA1–P_ERA4). Since the RMS errors shown in Table 1 are significantly larger than the amplitudes of the annual cycles in the errors, the variation of the errors in pressure–ZHD are not dominated by these seasonal cycles.

Figure 8 shows the time series of the errors in P_GPT2w and P_ERA1 and the seasonal cycles (Eq. 15) estimated from the time series for station JPLM (34.2° N, 118.2° W; in the Northern Hemisphere) and station SUTM (32.8° S, 20.8° E; in the Southern Hemisphere). We can see that although the seasonal cycles in the time series of the errors in P_GPT2w are quite small, compared to the magnitude of the errors, the magnitudes of the errors at these two stations show a very obvious dependence on season. This shows that the errors in GPT2w-derived pressure–ZHD at JPLM are noticeably larger in December–February (i.e., winter in the Northern Hemisphere) than that in June–August. In contrast, the errors in the GPT2w-derived pressure–ZHD at SUTM are obviously larger in June–August (i.e., winter in the Southern Hemisphere) than that in December–February. This means that the RMSEs of the GPT2w-derived pressure–ZHD at these two stations are larger in the cold season than in the warm season. The results at all 76 stations show that the RMSEs of P_GPT2w in the cold season are 1.7 times those in the warm season in the high-latitude belt, 1.8 times in mid-latitude and 1.2 times in low-latitude. This also explains why

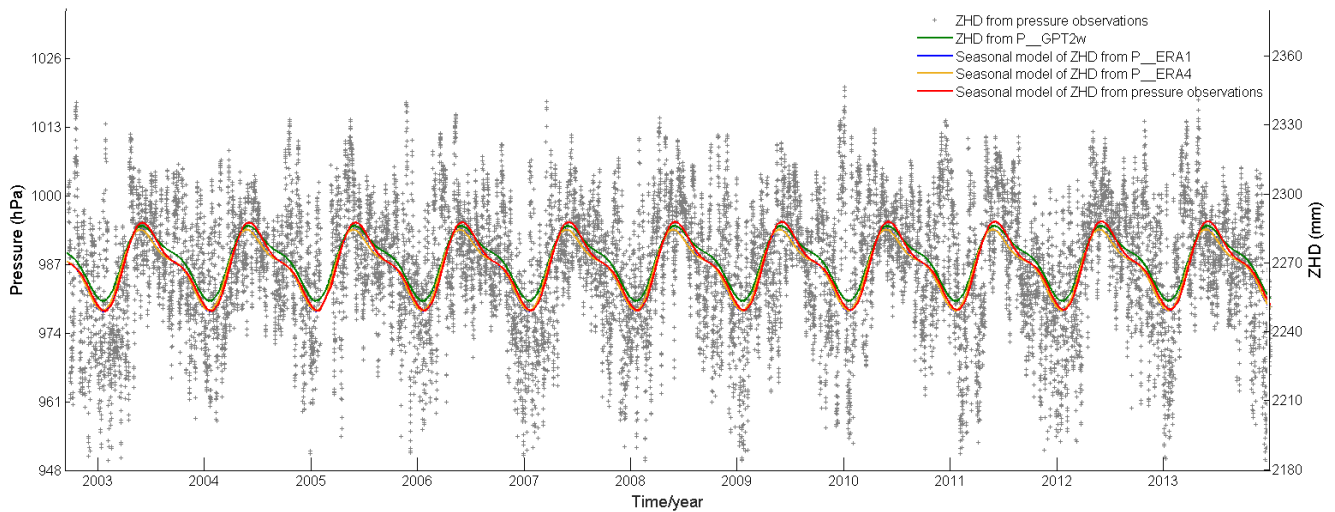


Figure 5. Comparison among the ZHD derived from P_GPT2w and seasonal models (annual and semiannual cycles) estimated from P_ERA1, P_ERA4 and pressure observations at station QAQ1 (60.8° N, 45.1° W).

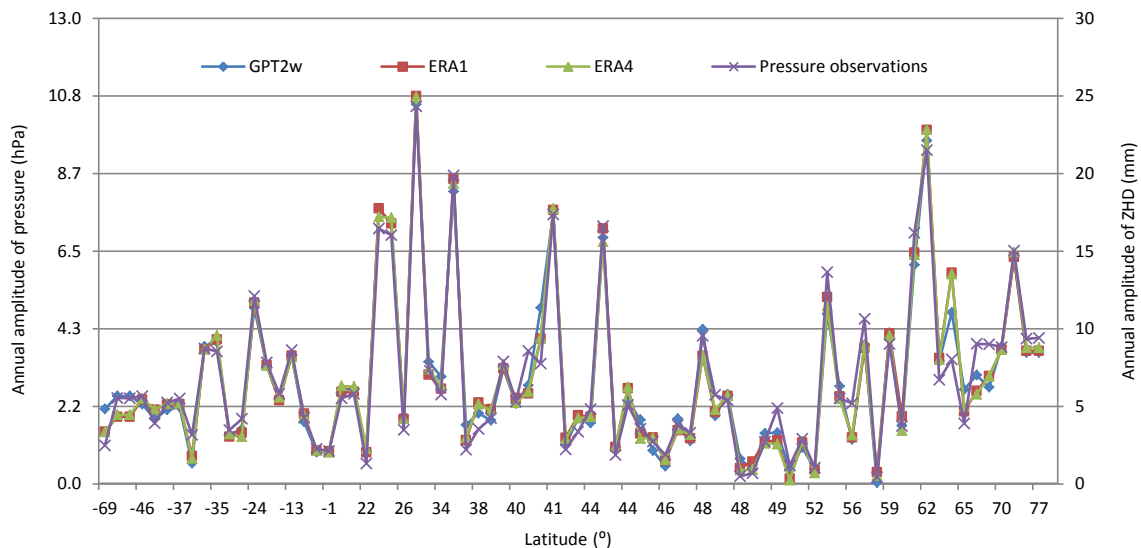


Figure 6. Annual amplitudes of the ZHD derived from P_GPT2w, P_ERA1, P_ERA4 and pressure observations at 76 stations.

large errors are found in the GPT2w-derived IWV at low IWV values (Fig. 4) in mid- and high-latitude belts since low IWV values are usually expected in the cold season, when P_GPT2w has a larger error.

4 Conclusions

The lack of meteorological data makes it very difficult to take full advantage of historical GNSS data for climate studies. This research is part of our continuous effort to extend our research presented in Wang et al. (2016a) by investigating the alternative methods for the determination of ZHD and developing of a new global long-term IWV time series, which

is critical for an improved understanding of climate change using the state of the art GNSS technology.

In this study, the accuracies of the ERA-Interim-derived surface pressure (calculated from the nearest grid point and interpolated from four surrounding grid points) and GPT2w-derived 6 h pressure have been investigated by comparing them against the observed pressure for 108 stations during the period 2000–2013. The biases of both ERA-Interim-derived and GPT2w-derived pressures are between -1 and 1 hPa at most stations. For those stations located in low-latitude regions, the RMSEs of GPT2w-derived 6 h pressure values are in the range of 1.0 to 4.3 hPa with a mean of 2.5 hPa. However, for the stations located in the mid-latitude belts, the mean value of the RMSEs is 7.3 hPa, and for the

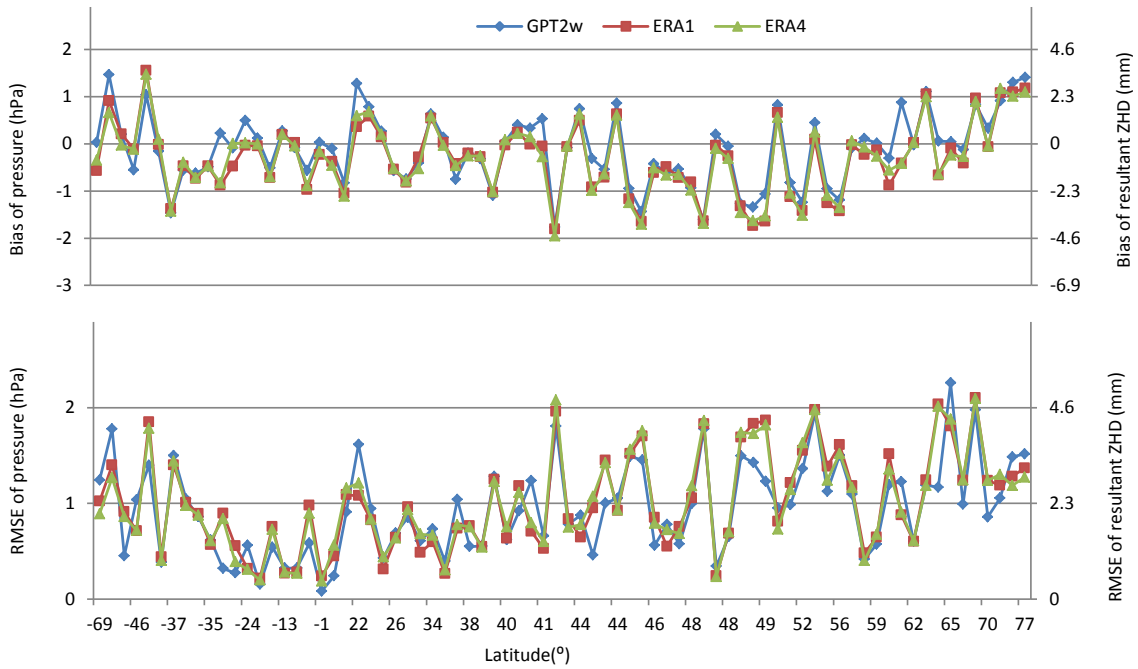


Figure 7. Bias of P_GPT2w and pressure derived from the seasonal models (annual and semiannual cycles) estimated from P_ERA1 and P_ERA4 time series (seasonal model derived from surface observations was used as a reference).

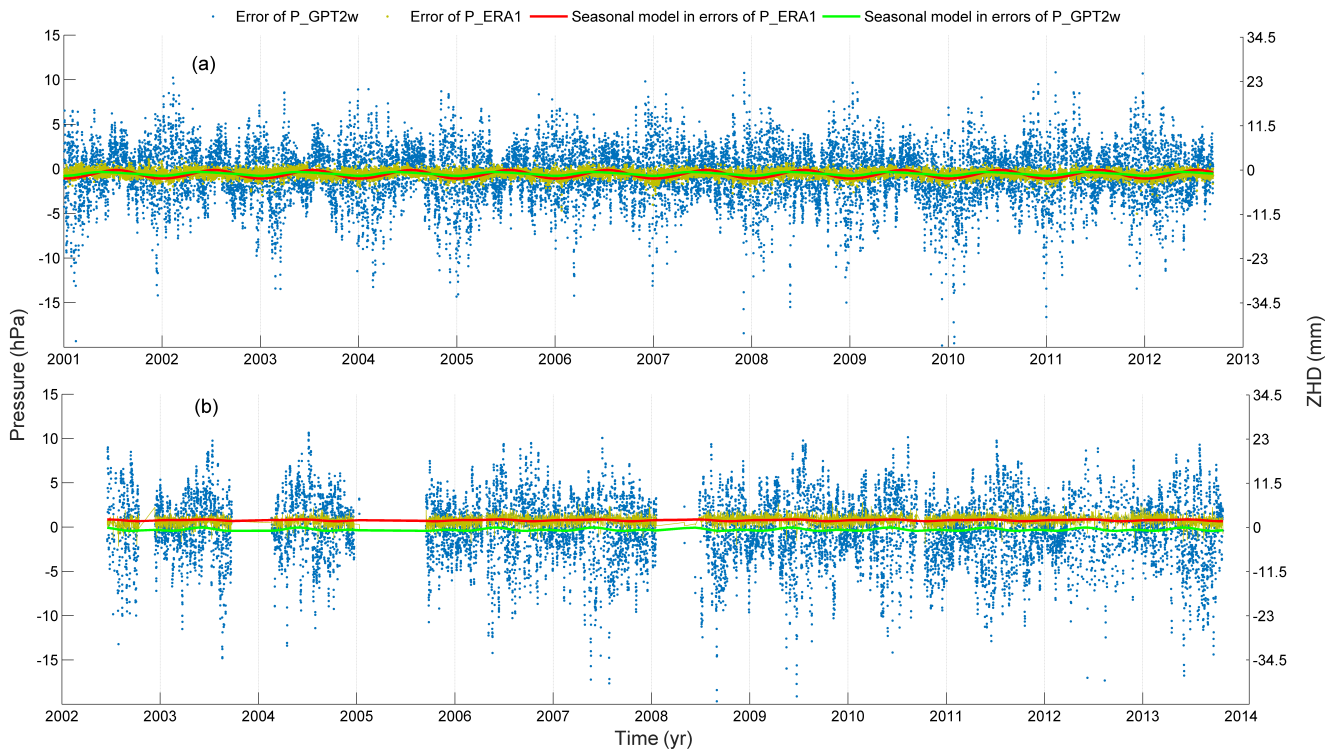


Figure 8. Time series of errors in pressure for stations JPLM (a 34.2° N, 118.2° W) and SUTM (b 32.8° S, 20.8° E) and the seasonal models estimated from the errors.

stations located in the high-latitude belts, the mean of the RMSEs is 9.9 hPa. The RMSEs of the two sets of ERA-Interim-derived pressure at all the 108 stations are both in the range of 0.2 to 4.0 hPa, and the mean value is 0.7 hPa in the low-latitude region and 1.0 hPa in the other regions. In terms of RMSE, a 1 hPa error in the determined pressure will lead to a 2.3 mm error in its resultant ZHD and about 0.35 kg m^{-2} in its resultant IWV. Therefore, the characteristics of the spatial distribution of the RMSE in ZHD and IWV are similar to those of pressure. The biases of ZHD and IWV from both ERA-Interim and GPT2w are in the range of -2.3 to 2.3 mm and -0.35 to 0.35 kg m^{-2} at most stations, respectively. In addition, the study also indicates that the RMSEs of the three sets of pressure and ZHD are all noticeably larger in the cold season than that in the warm season.

Results show that the mean relative error in the monthly IWV resulting from ERA-Interim-derived pressure across 99 stations is about 1.6%. However, the relative error in the GPT2w-derived IWV reaches as high as 6.7% in the mid-latitude region and even 21.5% in the high-latitude regions. This suggests that monthly IWV determined using ERA-Interim-derived pressure has a good accuracy and thus has the potential to be used for climate studies. The good agreement between the pressure derived from GPT2w and seasonal models estimated from pressure observations and ERA-Interim indicates that GPT2w captures the seasonal variations in pressure very well.

Data availability. Our new IWV dataset across 371 stations for the period of 2000–2013 has been made available at <https://doi.org/10.1594/PANGAEA.862525> (Wang et al., 2016b). It should be noted that this IWV dataset is not homogenized and probably not suitable to be directly used for retrieving long-term linear trends from them. The ERA-Interim-derived surface pressure and ZHD is available at <https://sites.google.com/site/zhddata/data>.

The Supplement related to this article is available online at <https://doi.org/10.5194/amt-10-2807-2017-supplement>.

Competing interests. The authors declare that they have no conflict of interest.

Special issue statement. This article is part of the special issue “Advanced Global Navigation Satellite Systems tropospheric products for monitoring severe weather events and climate (GNSS4SWEC) (AMT/ACP/ANGEo inter-journal SI)”. It does not belong to a conference.

Acknowledgements. This project is funded by the National Key Research and Development Plan (no. 2016YFB0501405),

the Australian Research Council (ARC) Linkage RMIT High Degree by Research Publications Grant (HDRPG), (LP0883288) projects, the China Scholarship Council (CSC), the National Key Research Program of China “Collaborative Precision Positioning Project” (no. 2016YFB0501900), China Natural Science Funds (nos. 41304034, 41674043, C41621063), the Beijing Nova Program (no. xx2017042), and the National High-tech R&D Program of China (no. 2014AA123503). We thank the Center for Orbit Determination in Europe for providing the zenith total delay results, the European Centre for Medium-Range Weather Forecasts for providing the ERA-Interim reanalysis, and the Scripps Orbit and Permanent Array Center for providing the surface pressure measurements. We also thank Johannes Böhm for providing the GPT2w model. We appreciate PANGAEA’s help in publishing our new IWV dataset, especially the help from Stefanie Schumacher and Rainer Sieger. We are grateful for the constructive comments from Olivier Bock and three anonymous reviewers.

Edited by: Olivier Bock

Reviewed by: Olivier Bock and two anonymous referees

References

- Bevis, M., Businger, S., Herring, T. A., Rocken, C., Anthes, R. A., and Ware, R. H.: GPS meteorology: Remote sensing of atmospheric water vapor using the Global Positioning System, *J. Geophys. Res.-Atmos.*, 97, 15787–15801, 1992.
- Bevis, M., Businger, S., Chiswell, S., Herring, T. A., Anthes, R. A., Rocken, C., and Ware, R. H.: GPS meteorology: Mapping zenith wet delays onto precipitable water, *J. Appl. Meteorol.*, 33, 379–386, 1994.
- Bianchi, C. E., Mendoza, L. P. O., Fernández, L. I., Natali, M. P., Meza, A. M., and Moirano, J. F.: Multi-year GNSS monitoring of atmospheric IWV over Central and South America for climate studies, *Ann. Geophys.*, 34, 623–639, <https://doi.org/10.5194/angeo-34-623-2016>, 2016.
- Bock, O. and Doerflinger, E.: Atmospheric modeling in GPS data analysis for high accuracy positioning, *Phys. Chem. Earth Pt. A*, 26, 373–383, 2001.
- Bock, O. and Nuret, M.: Verification of NWP model analyses and radiosonde humidity data with GPS precipitable water vapor estimates during AMMA, *Weather Forecast.*, 24, 1085–1101, 2009.
- Bock, O., Bosser, P., Bourcy, T., David, L., Goutail, F., Hoareau, C., Keckhut, P., Legain, D., Pazmino, A., Pelon, J., Pipis, K., Poujol, G., Sarkissian, A., Thom, C., Tournois, G., and Tzanos, D.: Accuracy assessment of water vapour measurements from in situ and remote sensing techniques during the DEMEVAP 2011 campaign at OHP, *Atmos. Meas. Tech.*, 6, 2777–2802, <https://doi.org/10.5194/amt-6-2777-2013>, 2013.
- Böhm, J., Heinkelmann, R., and Schuh, H.: Short note: a global model of pressure and temperature for geodetic applications, *J. Geodesy*, 81, 679–683, 2007.
- Böhm, J. and Schuh, H.: Atmospheric effects in space geodesy, Springer, 2013.
- Böhm, J., Möller, G., Schindelegger, M., Pain, G., and Weber, R.: Development of an improved empirical model for slant delays in the troposphere (GPT2w), *GPS Solutions*, 3, 433–441, 2015.

- Bokoye, A., Royer, A., O'Neill, N., Cliche, P., McArthur, L., Teillet, P., Fedosejevs, G., and Thériault, J. M.: Multi-sensor analysis of integrated atmospheric water vapor over Canada and Alaska, *J. Geophys. Res.-Atmos.*, 108, 4480, <https://doi.org/10.1029/2002JD002721>, 2003.
- Davis, J., Herring, T., Shapiro, I., Rogers, A., and Elgered, G.: Geodesy by radio interferometry: Effects of atmospheric modeling errors on estimates of baseline length, *Radio Sci.*, 20, 1593–1607, 1985.
- Dee, D., Uppala, S., Simmons, A., Berrisford, P., Poli, P., Kobayashi, S., Andrae, U., Balmaseda, M., Balsamo, G., and Bauer, P.: The ERA-Interim reanalysis: Configuration and performance of the data assimilation system, *Q. J. Roy. Meteor. Soc.*, 137, 553–597, 2011.
- Elgered, G., Davis, J., Herring, T., and Shapiro, I.: Geodesy by radio interferometry: Water vapor radiometry for estimation of the wet delay, *J. Geophys. Res.-Sol. Ea.*, 96, 6541–6555, 1991.
- Guerova, G., Jones, J., Douša, J., Dick, G., de Haan, S., Pottiaux, E., Bock, O., Pacione, R., Elgered, G., Vedel, H., and Bender, M.: Review of the state of the art and future prospects of the ground-based GNSS meteorology in Europe, *Atmos. Meas. Tech.*, 9, 5385–5406, <https://doi.org/10.5194/amt-9-5385-2016>, 2016.
- Heise, S., Dick, G., Gendt, G., Schmidt, T., and Wickert, J.: Integrated water vapor from IGS ground-based GPS observations: initial results from a global 5-min data set, *Ann. Geophys.*, 27, 2851–2859, <https://doi.org/10.5194/angeo-27-2851-2009>, 2009.
- ICAO: Manual of the ICAO Standard Atmosphere (extended to 80 kilometres (262 500 feet)), International Civil Aviation Organization Montreal 92-9194-004-6, 1993.
- Janjić, T. and Cohn, S. E.: Treatment of observation error due to unresolved scales in atmospheric data assimilation, *Mon. Weather Rev.*, 134, 2900–2915, 2006.
- Jin, S. and Luo, O.: Variability and climatology of PWV from global 13-year GPS observations, *IEEE T. Geosci. Remote*, 47, 1918–1924, 2009.
- Kleijer, F.: Troposphere modeling and filtering for precise GPS leveling, TU Delft, Delft University of Technology, 2004.
- Kumar, S., Singh, A., Prasad, A. K., and Singh, R.: Variability of GPS derived water vapor and comparison with MODIS data over the Indo-Gangetic plains, *Phys. Chem. Earth*, 55, 11–18, 2013.
- Lagler, K., Schindelegger, M., Bohm, J., Krasna, H., and Nilsson, T.: GPT2: Empirical slant delay model for radio space geodetic techniques, *Geophys. Res. Lett.*, 40, 1069–1073, <https://doi.org/10.1002/grl.50288>, 2013.
- Li, X., Dick, G., Ge, M., Heise, S., Wickert, J., and Bender, M.: Real-time GPS sensing of atmospheric water vapor: Precise point positioning with orbit, clock, and phase delay corrections, *Geophys. Res. Lett.*, 41, 3615–3621, 2014.
- Li, X., Zus, F., Lu, C., Dick, G., Ning, T., Ge, M., Wickert, J., and Schuh, H.: Retrieving of atmospheric parameters from multi-GNSS in real time: Validation with water vapor radiometer and numerical weather model, *J. Geophys. Res.-Atmos.*, 120, 7189–7204, 2015.
- Musa, T. A., Amir, S., Othman, R., Ses, S., Omar, K., Abdullah, K., Lim, S., and Rizos, C.: GPS meteorology in a low-latitude region: Remote sensing of atmospheric water vapor over the Malaysian Peninsula, *J. Atmos. Sol.-Terr. Phy.*, 73, 2410–2422, 2011.
- Niell, A., Coster, A., Solheim, F., Mendes, V., Toor, P., Langley, R., and Upham, C.: Comparison of measurements of atmospheric wet delay by radiosonde, water vapor radiometer, GPS, and VLBI, *J. Atmos. Ocean. Technol.*, 18, 830–850, 2001.
- Nilsson, T. and Elgered, G.: Long-term trends in the atmospheric water vapor content estimated from ground-based GPS data, *J. Geophys. Res.-Atmos.*, 113, D19101, <https://doi.org/10.1029/2008JD010110>, 2008.
- Ning, T. and Elgered, G.: Trends in the atmospheric water vapor content from ground-based GPS: The impact of the elevation cut-off angle, *IEEE J. Sel. Top. Appl.*, 5, 744–751, 2012.
- Norazmi, M. F. B., Opaluwa, Y. D., Musa, T. A., and Othman, R.: The Concept of Operational Near Real-Time GNSS Meteorology System for Atmospheric Water Vapour Monitoring over Peninsular Malaysia, *Arab. J. Sci. Eng.*, 40, 235–244, 2015.
- Offiler, D.: Product requirements document version 1.0–21 December 2010, EIG EUMETNET GNSS Water Vapour Programme (E-GVAP-II), 2010.
- Rohm, W., Yuan, Y. B., Biadeglne, B., Zhang, K. F., and Le Marshall, J.: Ground-based GNSS ZTD/IWV estimation system for numerical weather prediction in challenging weather conditions, *Atmos. Res.*, 138, 414–426, <https://doi.org/10.1016/j.atmosres.2013.11.026>, 2014.
- Ross, R. J. and Rosenfeld, S.: Estimating mean weighted temperature of the atmosphere for Global Positioning System applications, *J. Geophys. Res.-Atmos.*, 102, 21719–21730, 1997.
- Saastamoinen, J.: Atmospheric correction for the troposphere and stratosphere in radio ranging satellites, in: The use of artificial satellites for geodesy, Washington: American Geophysical Union, 247–251, 1972.
- Schneider, M., Romero, P. M., Hase, F., Blumenstock, T., Cuevas, E., and Ramos, R.: Continuous quality assessment of atmospheric water vapour measurement techniques: FTIR, Cimel, MFRSR, GPS, and Vaisala RS92, *Atmos. Meas. Tech.*, 3, 323–338, <https://doi.org/10.5194/amt-3-323-2010>, 2010.
- Tetens, O.: Über einige meteorologische Begriffe, *Z. Geophys.*, 6, 297–309, 1930.
- Vonder Haar, T. H., Bytheway, J. L., and Forsythe, J. M.: Weather and climate analyses using improved global water vapor observations, *Geophys. Res. Lett.*, 39, L15802, <https://doi.org/10.1029/2012GL052094>, 2012.
- Wang, J., Zhang, L., and Dai, A.: Global estimates of water-vapor-weighted mean temperature of the atmosphere for GPS applications, *J. Geophys. Res.-Atmos.*, 110, D21101, <https://doi.org/10.1029/2005JD006215>, 2005.
- Wang, J., Zhang, L., Dai, A., Van Hove, T., and Van Baelen, J.: A near-global, 2 h data set of atmospheric precipitable water from ground-based GPS measurements, *J. Geophys. Res.-Atmos.*, 112, D11107, <https://doi.org/10.1029/2006JD007529>, 2007.
- Wang, X., Zhang, K., Wu, S., Fan, S., and Cheng, Y.: Water vapor-weighted mean temperature and its impact on the determination of precipitable water vapor and its linear trend, *J. Geophys. Res.-Atmos.*, 121, 833–852, <https://doi.org/10.1002/2015jd024181>, 2016a.
- Wang, X., Zhang, K., Wu, S., Fan, S., and Cheng, Y.: Long-term global GPS-derived precipitable water vapor data set, RMIT University, Melbourne, PANGAEA, <https://doi.org/10.1594/PANGAEA.862525>, 2016b.

- Wilgan, K., Rohm, W., and Bosy, J.: Multi-observation meteorological and GNSS data comparison with Numerical Weather Prediction model, *Atmos. Res.*, 156, 29–42, 2015.
- Yao, Y., Zhu, S., and Yue, S.: A globally applicable, season-specific model for estimating the weighted mean temperature of the atmosphere, *J. Geodesy*, 86, 1125–1135, 2012.
- Yao, Y., Xu, C., Zhang, B., and Cao, N.: A global empirical model for mapping zenith wet delays onto precipitable water vapor using GGOS Atmosphere data, *Science China Earth Sciences*, 58, 1361–1369, 2015.
- Zhang, H., Pu, Z., and Zhang, X.: Examination of errors in near-surface temperature and wind from WRF numerical simulations in regions of complex terrain, *Weather Forecast.*, 28, 893–914, 2013.
- Zhang, K., Manning, T., Wu, S., Rohm, W., Silcock, D., and Choy, S.: Capturing the Signature of Severe Weather Events in Australia Using GPS Measurements, *IEEE J. Sel. Top. Appl.*, 8, 1839–1847, <https://doi.org/10.1109/jstars.2015.2406313>, 2015.